Food Hydrocolloids 126 (2022) 107456

Contents lists available at ScienceDirect

Food Hydrocolloids

journal homepage: www.elsevier.com/locate/foodhyd

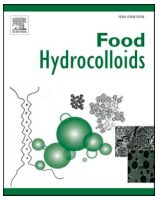

Optimizing pea protein fractionation to yield protein fractions with a high foaming and emulsifying capacity

Remco Kornet [a,b,1], Jack Yang [a,b,c,1], Paul Venema [b,*], Erik van der Linden [b], Leonard M. C. Sagis [b]

[a] TiFN, P.O. Box 557fir, 6700 AN, Wageningen, the Netherlands
[b] Laboratory of Physics and Physical Chemistry of Foods, Wageningen University, Bornse Weilanden 9, 6708 WG, Wageningen, the Netherlands
[c] Laboratory of Biobased Chemistry and Technology, Wageningen University, Bornse Weilanden 9, 6708 WG, Wageningen, the Netherlands

ARTICLE INFO

Keywords:
Pea protein
Albumin
Globulin
Surface rheology
Foam
Emulsion

ABSTRACT

Specific pea protein fractionation steps can be used to control foaming and emulsifying properties of three pea protein fractions at pH 7.0. Mild fractionation, involving dispersion of the flour at pH 8.0, subsequent centrifugation, and drying of the supernatant yielded a pea protein concentrate (PPC). Further fractionation was achieved by applying isoelectric precipitation on the supernatant, followed by centrifugation, and re-dispersion, resulting in the globulin-rich fraction (GLB-RF); the supernatant – which could be considered a by-product – was diafiltrated to obtain the albumin-rich fraction (ALB-RF). Size exclusion chromatography showed that PPC contained mostly globulins and some albumins, whereas GLB-RF and ALB-RF indeed contained either globulins or albumins. The smaller and less charged albumins displayed strong in-plane interactions at the air-water interface, thereby forming a stiff and cohesive interfacial layer which led to high foam overrun (258%) and stability (272 min). PPC- and GLB-RF contained larger and highly charged globulins, showing substantially lower foam overruns (<81%) and stability (<70 min), which can be attributed to the formation of weaker and more mobile interfacial layers than ALB-RF. For the emulsifying properties, it was found that the larger size and higher net charge of globulins resulted in the formation of oil droplets that were stable against coalescence and flocculation, while albumin-stabilised oil droplets flocculated due to lower surface charges. The functionality of the fraction is largely determined by the protein composition. We have demonstrated how targeted fractionation can be used to control this composition, and hence the functionality of pea protein fractions.

1. Introduction

For sustainability reasons, there is an ongoing shift from animal-to plant-based proteins in food applications. Pea is one of the plant protein sources that is commercially used to produce protein concentrates and isolates, and has also been subject of many studies. Advantages of pea protein compared with proteins from other legumes are that it has a low allergenicity and quite a complete essential amino acid profile (Boukid, Rosell, & Castellari, 2021; Burger & Zhang, 2019). To utilise the proteins that pea has to offer, it is common practice to process pea seeds into pure protein-fractions. Aqueous or wet fractionation is the mainstream process and can yield high protein purities (Schutyser & van der Goot, 2011). Such a process is based on solubilisation and subsequent isoelectric precipitation, with intermediate centrifugation steps, to obtain a protein-rich fraction. The drawback of such a process is the requirement of copious amounts of energy and water. Therefore, milder fractionation methods have been developed, such as dry fractionation and mild wet fractionation (Assatory, Vitelli, Rajabzadeh, & Legge, 2019; Möller, van der Padt, & van der Goot, 2020). Generally, these processes have a lower environmental impact, but also yield fractions with lower protein purities (Lie-Piang, Braconi, Boom, & van der Padt, 2021).

An alternative way of looking at milder fractionation is to limit the number of fractionation steps in a conventional aqueous fractionation process. An advantage of fewer processing steps is a less radical change with respect to the current plant protein manufacturing process. Limited fractionation yields fractions with a more heterogenous composition, caused by components such as sugars, salts, phenols and oil. On the

* Corresponding author.
E-mail address: paul.venema@wur.nl (P. Venema).
[1] These authors have contributed equally to this work.

https://doi.org/10.1016/j.foodhyd.2021.107456
Received 29 July 2021; Received in revised form 14 December 2021; Accepted 15 December 2021
Available online 16 December 2021

other hand, mildly fractionated protein concentrates were found to possess better overall functionality compared to extensively fractionated ones (Geerts, Mienis, Nikiforidis, van der Padt, & van der Goot, 2017; Sridharan, Meinders, Bitter, & Nikiforidis, 2020), as milder processed fractions are more likely to preserve the native properties of the proteins. Additionally, the protein composition, influenced by the fractionation steps used, can be optimized for specific functional behaviour.

Previous research demonstrated that fractionation could affect functional properties of pea protein, as we observed a better gelling capacity for limitedly fractionated samples (Kornet et al., 2021), and found that the protein composition and viscosity of the fractions can be altered by the extent of fractionation (Kornet et al., 2020). In the latter study, three different protein fractions could be obtained from a conventional aqueous fractionation process: an albumin-enriched fraction, a globulin-enriched fraction and a fraction with both globulins and albumins. The separation of these proteins is based on the characteristic of globulins to precipitate around pH 4.5 (Boye, Zare, & Pletch, 2010; Lam, Can Karaca, Tyler, & Nickerson, 2016), while albumins remain soluble (S. Yang, Li, et al., 2020). The three protein fractions – either containing albumins, globulins or both - were already found to show different solubilities, protein specific volumes, and viscosities. It is not yet understood how other types of functional behaviour – such as foaming and emulsifying properties – are affected by pea protein fractionation processes, which will be elaborately studied in this work.

Foaming or emulsifying properties are essential to produce certain types of foods. These functionalities could be provided by plant proteins after an optimized protein fractionation. Mildly fractionated pea proteins have received some attention with respect to emulsion stabilising properties (Ghumman, Kaur, & Singh, 2016; Sridharan et al., 2020), but a comprehensive study on the interface- and foam-stabilising properties does not exist. Extensively fractionated pea proteins have been studied, but the majority of these studies focus on a globulin-enriched fraction (Barac et al., 2010; Karaca, Low, & Nickerson, 2011; Kimura et al., 2008; Taherian et al., 2011), whereas the functionality studies on a pea albumin-enriched fraction were found to be limited to one study (Lu, Quillien, & Popineau, 2000).

Here, we aim to compare mild and extensively processed pea protein fractions with different protein compositions (i.e., albumins, globulins, or both) on their foaming and emulsifying properties. We hypothesized that albumins and globulins display different foaming and emulsifying properties, as both proteins substantially differ in their molecular properties, such as size, hydrophobicity and charge (Kornet et al., 2021). These protein molecular properties can largely affect interfacial, foam and emulsion stabilising properties, which could result in pronounced differences between albumins and globulins. The protein fractions were studied by a multi-length scale approach, where the molecular properties (protein size, charge and structure) were linked to the macroscopic properties (foam and emulsion). Firstly, we characterized the pea protein fractions on composition and physical properties such as viscosity, charge and thermal properties. The viscosity and charge were analysed because they may affect foam and emulsion stability, while the thermal properties were analysed to verify that the fractionation processes did not induce protein denaturation. Secondly, we studied the foaming and emulsifying properties as well as the air – water interfacial properties of the pea protein fractions. By using such an approach, we demonstrate how pea can be fractionated to yield protein-enriched fractions with optimal foaming and emulsifying properties. The implementation of such fractionation techniques could increase the potential of plant proteins as functional ingredients, and simultaneously increase the resource efficiency of peas.

2. Experimental section

2.1. Materials

Yellow pea (Pisum Sativum L.) seeds were obtained from Alimex Europe BV (Sint Kruis, The Netherlands). Rapeseed oil was obtained from Danone Nutricia Research (Utrecht, the Netherlands). All chemicals and reagents were obtained from Merck (Darmstadt, Germany) and were of analytical grade. All samples were prepared in ultrapure water (MilliQ Purelab Ultra, Germany), unless stated otherwise.

2.2. Protein fractionation process

An aqueous fractionation process based on Kornet et al. (2020), and visualized in Fig. 1, was used to produce three protein-rich fractions. Pea was milled into flour with an average particle size of 100 μm. The flour was dispersed in deionised water in a ratio of 1:10 and the pH was adjusted to 8.0 using 1 M NaOH. Proteins and other flour constituents were solubilized for 2 h under moderate stirring. Subsequently, the soluble components were separated from the insoluble components by centrifugation (10.000×*g*, 30 min, 20 °C). Part of the resulting supernatant was lyophilised and labelled as pea protein concentrate (PPC). The remainder was adjusted to pH 4.5 using 1 M HCl to precipitate the globulins, and kept there for 2 h under moderate stirring. The precipitated globulins were separated from the soluble albumins by centrifugation (10.000×*g*, 30 min, 20 °C). The resulting supernatant and pellet were separated, and the supernatant was diafiltrated using a 2 kDa membrane. The retentate was lyophilised and labelled as the albumin-rich fraction (ALB-RF). The pellet, containing the precipitated globulins, was re-dispersed at pH 7.0 for 2 h and lyophilised afterwards.

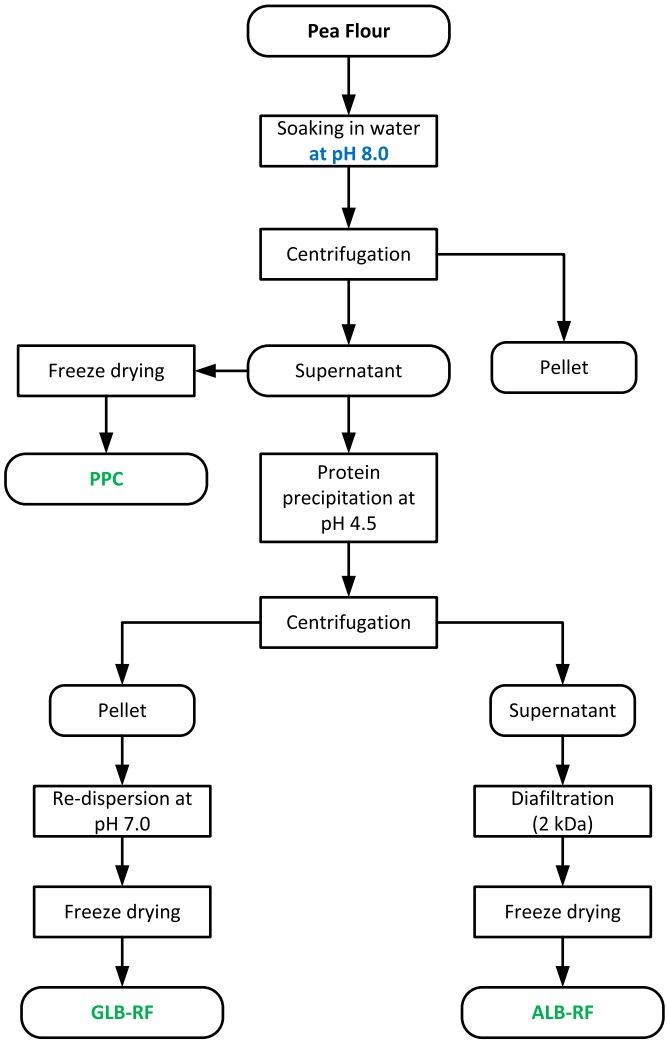

Fig. 1. Schematic representation of the pea protein fractionation process.

This fraction was labelled as the globulin-rich fraction (GLB-RF). The labels ALB-RF and GLB-RF are based on protein composition analysis, which is discussed later in this work. All steps in this fractionation process were conducted at room temperature. Lyophilisation was done in an Alpha 2–4 LD plus freeze-dryer (Christ, Osterode am Harz, Germany) and the powders were stored at −18 °C.

The protein purity and major impurity (i.e. ash) was quantified as a basic characterization of the pea protein fractions. The ash content was determined by heating the samples overnight in a furnace 550 °C and expressed as the mass after heating divided by the initial mass minus the moisture content. The protein content was calculated from the nitrogen content, measured by a FLASH EA 1112 series Dumas (Interscience, Breda, The Netherlands) using a nitrogen conversion factor of 5.7. All protein purities have been expressed as the weight percentage of protein in total dry matter. The protein recovery (%) was defined as the protein quantity in the pea fraction divided over the protein quantity in the pea flour.

2.3. Pea fraction dissolution and pH standardization

All samples were dissolved in phosphate-buffer (20 mM, pH 7.0, mixture of Na_2HPO_4 and NaH_2PO_4), unless stated otherwise. Samples were stirred for at least 4 h at room temperature.

2.4. Size exclusion chromatography (SEC)

The protein composition of the pea protein fractions was determined by separation on an Akta Pure 25 chromatography system (GE Healthcare, Diegem, Belgium), and subsequently detected using an UV detector. Samples were prepared by dissolving 5 g protein/L in a McIlvaine buffer (10 mM citric acid, 20 mM Na2HPO4, pH 7.0, 150 mM NaCl, passed through a filter with a 45 μm pore size). The solutions were centrifuged at 3350×*g* for 10 min and the supernatants were transferred to HPLC (High Performance Liquid Chromatography) vials. The samples were run on a Superdex 200 increase 10/300 GL column (Merck, Schnelldorf, Germany) with a molecular weight range of 10–600 kDa, with the McIlvaine buffer used as an eluent. Proteins were detected at an UV wavelength of 280 nm. To determine the molecular masses, a calibration curve was used, obtained from molecules of known molecular weights: Aldolase (160 kDa), Blue Dextran (2000 kDa), Carbonic Anhydrase (290 kDa), Conalbumin (75 kDa), Ferritin (440 kDa), Ovalbumin (43 kDa) and Ribonuclease (14 kDa).

2.5. Differential scanning calorimetry (DSC)

The thermal properties of the pea protein fractions were measured with DSC, to gain understanding on the effect of fractionation on protein denaturation. Samples were prepared by dissolving 10% (w/w) protein in deionised water for 2 h and adjusted to pH 7.0. The protein solutions were transferred to high volume pans in weights of 30–40 mg. The pans were closed with a lid and measured with a TA Q200 Differential Scanning Calorimeter (TA Instruments, Etten-Leur, The Netherlands) with nitrogen as a cell purge gas. The heat flow was recorded over a temperature range of 20–120 °C, with a heating rate of 5 °C/min. All samples were measured in triplicate.

2.6. Determination of zeta-potential

The zeta-potential of 0.1% (w/w) proteins in phosphate buffer were determined using dynamic light scattering in a Zetasizer Nano ZS (Malvern Instruments, UK). The refractive indices were set on 1.45 for the proteins and 1.33 for the buffer phase. The measurements were performed in triplicates at 20 °C.

2.7. Capillary viscometry

The protein fractions were dispersed in concentrations of 0.1, 0.7 and 2.0% (w/w) protein, and the kinematic viscosities were measured with an Ubbelohde viscometer No. 1046928 (SI Analytics, Weilheim, Germany). These concentrations are identical to the concentrations at which the foams and emulsions were prepared (as mentioned in sections 2.12.1 and 2.13.2). The density of the solutions with different protein concentrations was measured with a density meter DMA5000 (Anton Paar, Graz, Austria). The kinematic viscosity was multiplied with the dispersion density to calculate the dynamic viscosity of the protein dispersions.

2.8. Determination of surface tension and surface dilatational moduli

The interfacial properties were studied by surface dilatational rheology using a drop tensiometer PAT-1M (Sinterface Technologies, Germany). Solutions containing 0.1% (w/w) protein were pumped through a needle to create a hanging droplet with a surface area of 20 mm^2. The droplet contour was captured by a camera and analysed by fitting the contour of the droplet with the Young-Laplace equation to obtain the surface tension. The interfaces were equilibrated for 3 h before starting the dilatational deformations. The amplitude dependence was studied in amplitude sweeps, where the amplitude of deformation was increased from 3 to 30% with 9 increments, while the frequency remained constant at 0.02 Hz. The frequency dependence was studied in frequency sweeps, where the frequency of an oscillation cycle was increased from 0.002 to 0.1 Hz with 7 increments, and the amplitude of deformation was constant at 3%. Each amplitude or frequency in the sweeps was performed with five oscillatory cycles, followed by a rest period with the same frequency. The relaxation response of the interfaces was studied by performing step-dilatations by a sudden compression or extension of 10% area change with a step time of 2 s. After the step, the area was kept constant for 1000 s. All experiments were performed at least in triplicate at 20 °C.

2.9. Interfacial rheological data analysis

From the amplitude sweeps, the raw data was analysed using Lissajous plots by plotting the surface pressure ($\Pi = \gamma\text{-}\gamma_0$) versus the relative surface deformation ($(A\text{-}A_0)/A_0$). Here, γ and A are the surface tension and area of the deformed interface, γ_0 and A_0 are the surface tension and area of the non-deformed interface. The middle three oscillations, of a total of five oscillations, were used to produce the plots.

2.10. Preparation of Langmuir-Blodgett films

A Langmuir trough (Langmuir-Blodgett Trough KN 2002, KSV NIMA/Biolin Scientific Oy, Finland) with an area of 243 mm^2 was used to produce Langmuir-Blodgett films of the protein interfaces. The trough was filled with phosphate buffer (20 mM, pH 7.0), and the surface pressure was measured with a Wilhelmy plate (platinum, perimeter 20 mm, height 10 mm). A total of 200 μL of 0.04% protein (w/w) solution was spread on top of the surface using a gas-tight syringe, followed by an equilibration step of 30 min. Afterwards, the interface was compressed by barriers at a moving speed of 5 mm/min. First, surface pressure isotherms were constructed, and based on these isotherms, two surface pressures (15 and 25 mN/m) were chosen to extract Langmuir-Blodgett films. The protein layer was transferred onto a freshly cleaved mica sheet (Highest Grade V1 Mica, Ted Pella, USA) at a speed of 1 mm/min. The films were produced in duplicate at 20 °C, and dried in a desiccator for further analysis.

2.11. Determination of the interfacial structure by AFM

The interfacial microstructure of the Langmuir-Blodgett films was

analysed using atomic force microscopy (AFM) on a Multimode 8-HR (Bruker, USA). The topographical measurement was performed with a Scanasyst-air model non-conductive pyramidal silicon nitride probe (Bruker, USA) with a normal spring constant of 0.40 mN/m, and images were recorded in tapping mode with a lateral frequency of 0.977 Hz. At least two areas of 2×2 μm^2 with a resolution of 512×512 $pixels^2$ on each replicate were analysed to ensure good representativeness. The images were analysed and processed using Nanoscope Analysis software v1.5 (Bruker, USA).

2.12. Determination of foaming properties

2.12.1. Foam ability

A whipping method was used to study the foam ability of a solution with a protein content of 0.1% (w/w). Aliquots of 15 mL sample were whipped in a plastic tube (3.4 cm internal diameter) for 2 min at 2000 rpm by an aerolatte froth (Aerolatte Ltd., UK) connected to an overhead stirrer. The top of the foam was marked on the tube, and the height of the foam was measured with a ruler. The foam height and tube diameter were used to calculate the foam volume. The overrun was calculated by equation (1).

$$Overrun\ (\%) = \frac{Foam\ volume\ (mL)}{Liquid\ volume\ (15\ mL)}\ x\ 100\% \quad (1)$$

All experiments were performed in triplicate at room temperature.

2.12.2. Foam stability

A sparging method was used to study the foam stability, as the initial foam height can be regulated in this method. Foams were sparged using nitrogen gas in a Foamscan foaming device (Teclis IT-concept, France). A glass cylinder with 60 mm diameter was filled with 60 mL of a 0.1% (w/w) protein solution. The gas was sparged through a metal frit (27 μm pore size, 100 μm distance between centres of pores, square lattice) at a gas flow rate of 400 mL/min to create a foam with a volume of 500 mL. The foam volume was analysed by a camera until half of the initial foam volume had collapsed, which is also known as the foam volume half-life time. Images of the air bubbles were also recorded and analysed using a custom made Matlab script with the DIPlip and DIPimage analysis software (TU Delft, Delft, the Netherlands), which calculated the average air bubble size. All experiments were at least performed in triplicate at 20 °C.

2.13. Determination of emulsifying properties

2.13.1. Removal of impurities in rapeseed oil

Surface-active impurities in rapeseed oil were removed using magnesium silicate (100–200 mesh Florisil, Sigma-Aldrich, USA). Florisil and rapeseed oil were mixed in a ratio of 1:2 (v/v) (Florisil:oil) in air-tight tubes. To prevent light oxidation, the tubes were covered with aluminium foil. Afterwards, the tubes were rotated overnight at room temperature. The following day, the sample was centrifuged twice at 2,000 g for 20 min to remove the pellet containing Florisil. The final supernatant, containing purified rapeseed oil, was recovered, and stored at −20 °C for further use.

2.13.2. Preparation of oil-in water emulsions

Oil-in-water emulsions were prepared with solutions containing 0.7 and 2% (w/w) protein. Purified rapeseed oil was added to a total oil content of 10% (w/w). The mixture (total 30 mL) was pre-homogenised with an Ultra-Turrax (IKA, USA) at 12,000 g for 1 min. The pre-emulsion was further homogenised in a high-pressure homogeniser (LAB, Delta Instruments, The Netherlands) at 200 bars for 10 passes at room temperature, while the emulsion beaker was cooled in ice water (±0 °C).

2.13.3. Determination of emulsion droplet size

Static light scattering in a Mastersizer 2000 (Malvern Instruments Ltd, UK) was used to determine the emulsion droplet size distribution. The droplet size distribution was measured directly after homogenisation (day 0), on day 1, and on day 7, while stored at 4 °C. Samples were carefully rotated before analysis, and aliquots of emulsion were taken from the middle of the tube. Potential flocculation was studied by measuring the droplet size distribution of a mixture containing 0.5 mL of emulsion with 0.5 mL of 1% (w/w) sodium dodecyl sulphate (SDS) solution. The refractive indices used for the dispersed phase (rapeseed oil) and dispersant (demineralised water) were 1.469 and 1.330, respectively (E. B. Hinderink, Münch, Sagis, Schroën, & Berton-Carabin, 2019). Measurements were performed in triplicate at room temperature.

2.13.4. Visualization of emulsion droplets

Emulsions were studied in an Axios 2 Plus light microscope (Carl Zeiss AG, Germany) using an objective lens with a 40x magnification capacity. Images were recorded using the Axiocam (Carl Zeiss AG, Germany), which was connected to the microscope.

2.13.5. Determination of emulsion creaming

Creaming was studied by filling a 15 mL tube (1.2 cm diameter) with 10 mL emulsion. The tubes were stored in a vibration free cabin. Images were taken on day 0, 1, and 7. The emulsions were also studied visually using a light source to evaluate the volume of the creamed layer. A creaming percentage (%) was determined by equation (2).

$$Creaming\ percentage(\%) = \frac{Volume\ of\ (bottom)\ serum\ layer\ (mL)}{Volume\ of\ emulsion\ (10\ mL)} x100\% \quad (2)$$

2.14. Statistical analysis

The analysis of variance was performed on the data using a one-way analysis of variance (ANOVA) and Duncan's test at $p \leq 0.05$ to evaluate the statistical significance between samples. SPSS 25.0 (SPSS Inc., USA) software was used to run the tests.

3. Results and discussion

3.1. Compositional and physical properties of the pea protein fractions

3.1.1. Fractionation process and fraction composition

The aqueous fractionation process yielded three pea protein fractions that varied in protein content, based on dumas measurements. Pea protein concentrate (PPC) and the albumin-rich fraction (ALB-RF) contained over 50% (w/w) protein, whereas the globulin-rich fraction (GLB-RF) contained 86% (w/w) protein. The lower protein purity of PPC is a consequence of fewer fractionation steps (i.e., alkaline extraction and centrifugation only). This PPC also had a higher protein recovery of 74.6%, compared with 54.4% for GLB-RF (Table 1). This protein recovery was calculated from the measured protein content in the pea protein fractions and in the pea flour. Generally, more extensive

Table 1
Protein recovery and dry matter composition of the pea protein concentrate (PPC), albumin-rich fraction (ALB-RF) and globulin-rich fraction (GLB-RF). Also the dry matter composition of pea flour is included. The protein recovery is defined as the recovered amount of protein divided over the amount of protein before fractionation. Values are presented as mean ± standard deviation; means within a column with the same superscript letter are not significantly different ($p > 0.05$).

Pea protein fraction	Protein recovery (%)	Protein content (% (w/w))	Ash content (% (w/w))
Pea flour	–	18.8 ± 0.19^{a}	3.7 ± 0.3^{a}
PPC	74.6 ± 0.8^{c}	54.8 ± 4.8^{b}	10.3 ± 2.1^{c}
ALB-RF	12.3 ± 0.7^{a}	52.0 ± 1.7^{b}	5.5 ± 1.2^{b}
GLB-RF	54.4 ± 2.8^{b}	86.3 ± 1.4^{c}	5.6 ± 0.5^{b}

fractionation (e.g. a combination of protein solubilisation and precipitation) results in higher purities and lower yields (Tenorio, Kyriakopoulou, Suarez-Garcia, van den Berg, & van der Goot, 2018), due to protein losses throughout the process. This is also reflected in the sum of the ALB-RF and GLB-RF protein recovery (66.7%), which is lower than the protein recovery of PPC (74.6%), from which ALB-RF and GLB-RF originate. In other words, there is 7.9% loss of protein after isoelectric precipitation, probably due to incomplete removal of the protein from the centrifugation tubes. The low recovery of ALB-RF could be explained by the low albumin content in pea seeds, which comprised only 13–30% of the total protein content (Casey, Sharman, Wright, Bacon, & Guldager, 1982). The major impurities of PPC and ALB-RF were soluble sugars (e.g. pea raffinose and stachyose), based on earlier research on similar pea protein fractions (Kornet et al., 2020). The ash contents (Table 1) reflect the amounts of the second largest impurity. PPC contained around 10% ash, whereas ALB-RF and GLB-RF contained about 5%. The lower ash contents of ALB-RF and GLB-RF can be attributed to a diafiltration and a precipitation step, respectively. The results of this section do not only detail the efficiency of the fractionation processes but are also relevant to understand the foaming and emulsifying properties. A higher ash content implies a higher ionic strength. This most likely leads to enhanced screening of the protein charge and a reduced electrostatic repulsion between proteins.

3.1.2. The type of proteins present in the pea protein fractions

The SEC chromatogram (Fig. 2) shows the presence of proteins with higher molecular weights in PPC and GLB-RF, corresponding to the globulins. Globulins can be classified into legumin (11S) and vicilin (7S), and debatably to a third group called convicilin (Barac et al., 2010). The latter can also be considered as α-subunit of vicilin (O'Kane, Happe, Vereijken, Gruppen, & van Boekel, 2004). At pH 7.0, legumin is mostly present as a hexamer with a molecular weight ranging from 320 to 380 kDa. This hexamer comprises of six subunits that are non-covalently bound. Each of these subunits consist of an acidic and basic subunit of 40 kDa and 20 kDa. Vicilin is commonly present as a trimer with a molecular weight of 170 kDa. Convicilin has a subunit of ~70 kDa and it has a molecular weight of ~290 kDa in its native form (Barac et al., 2010; Croy, Gatehouse, Tyler, & Boulter, 1980). Based on these molecular weights, the first peak in the chromatogram (Fig. 2) can be denoted as legumin in its hexameric form (L), the second peak as convicilin (CV) and the third peak as vicilin (V). These proteins are absent in ALB-RF.

Albumin represents a group of proteins that includes PA1 (Pea Albumin), PA2, lectin, and protease inhibitors (Park, Kim, & Baik, 2010).

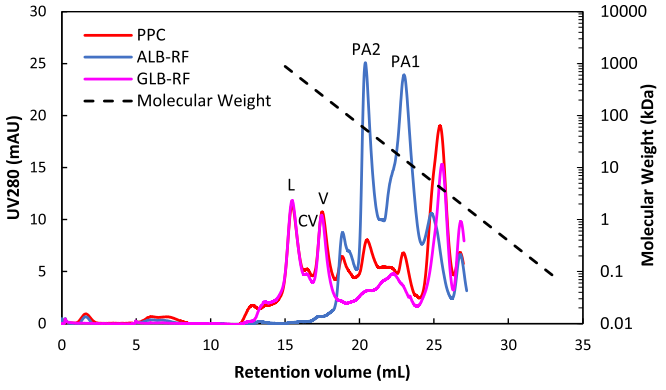

Fig. 2. Size Exclusion Chromatography (SEC) chromatogram showing the protein composition of the pea protein concentrate (PPC), albumin-rich fraction (ALB-RF) and globulin-rich fraction (GLB-RF), measured from 5 g/L protein solutions at pH 7.0. L = legumin, CV = convicilin, V = vicilin, PA1 and PA2 = albumins PA1 and PA2. For the UV detector a wavelength of 280 nm was used, and the signal intensity (arbitrary units) is shown on the y-axis. The black dashed line represents the molecular weight as function of retention volume.

PA1 can be subdivided into PA1a (6 kDa) and PA1b (4 kDa), and these polypeptides were previously suggested to be able to form dimers. Albumin PA2 comprises PA2a and PA2b that can form homodimers of 53 and 48 kDa, respectively (Higgins et al., 1986). Albumins PA1 and PA2 probably correspond to the major peaks of ALB-RF, as depicted in Fig. 2. Albumins are absent in GLB-RF, as they do not precipitate upon isoelectric precipitation (S. Yang, Li, et al., 2020). This means that in conventional processes the albumin proteins are generally discarded, despite of their potential as functional ingredient. Lower amounts of albumins are still present in PPC, but globulins remain the major protein, as globulins are more abundantly present in pea seeds.

The results of this section confirm that isoelectric precipitation results in a separation between albumins (ALB-RF) and globulins (GLB-RF). In later sections we will relate these compositional differences to differences in foaming and emulsifying properties.

3.1.3. Thermal properties

Previous studies have shown that pH shifts may denature the proteins, but this does not typically occur at pH 4.5 – the pH at which pea proteins are isoelectric precipitated (Arntfield & Murray, 1981; Shand, Ya, Pietrasik, & Wanasundara, 2007). In this study DSC measurements were conducted to determine the denaturation temperature and heat enthalpy, to confirm that the proteins were not denatured upon fractionation, as this could have strongly impacted functional behaviour. Denaturation peaks were observed, which implies that the proteins in all the fractions were – at least partially – native. Table 2 shows a denaturation temperature of 82.3 °C for the proteins in the GLB-RF. This is consistent with other values reported for pea globulins in literature, where denaturation temperatures (T_d) ranges between 75 and 85 °C (Lam et al., 2016; Mession, Sok, Assifaoui, & Saurel, 2013). Variation in denaturation temperatures in literature can be explained by different heating rates, presence of salts and sugars and different ratios of legumin versus vicilin. PPC shows a similar heat enthalpy as GLB-RF – probably because both fractions primarily contain globulins - and a slightly higher denaturation temperature (82.3 °C for GLB-RF and 85 °C for PPC). The latter could also be the result of a higher ash content (cf. Table 1). The ALB-RF displays the highest denaturation temperature and the lowest heat enthalpy. The denaturation profiles of pea albumins have not been studied previously, but the values reported in Table 2 correspond with earlier work on a less purified albumin fraction (Kornet et al., 2021). It appeared that, despite of higher number of cysteine residues in albumins (Higgins et al., 1986) and a compact structure that involves disulphide bonds (Park et al., 2010), thermal unfolding required less energy compared to larger pea globulins. The higher denaturation enthalpy of globulins is probably related to the larger and more complex globulin structure, and a higher number of interactions that stabilise the protein.

3.1.4. Viscosity

There are numerous factors influencing foam and emulsion stability, including air bubble or oil droplet size, protein adsorption behaviour, interfacial layer formation, and viscosity. The latter appeared to be a relevant characteristic for pea protein. That is why we studied the differences in viscosity of dispersions from the different pea protein

Table 2
Thermal denaturation properties of the pea protein concentrate (PPC), albumin-rich fraction (ALB-RF) and globulin-rich fraction (GLB-RF) in 10% (w/w) protein solutions at pH 7.0. Averages of the denaturation onset (T_{onset}), denaturation peak temperature (T_d) and heat enthalpy (ΔH_d) are given. Values are presented as mean ± standard deviation; means within a column with the same superscript letter are not significantly different ($p > 0.05$).

Pea protein fraction	T_{onset} (°C)	T_d (°C)	ΔH_d (J/g protein)
PPC	75.7 ± 0.2^b	85.0 ± 0.1^b	9.0 ± 0.2^b
ALB-RF	81.8 ± 0.0^c	87.7 ± 0.2^c	1.8 ± 0.1^a
GLB-RF	72.5 ± 0.2^a	82.3 ± 0.1^a	8.6 ± 0.4^b

fractions. Globulin-rich pea protein fractions have the ability to form aggregates that occupy large volumes in the system and hence display a significant thickening capacity (Kornet et al., 2020). The zero-shear viscosities of the pea protein fractions at concentrations of 0.1, 0.7 and 2.0% (w/w) protein were measured and displayed relative to the solvent viscosity (i.e., specific viscosity), in Fig. 3. We used the specific viscosities to show the contribution of the solute to the solution viscosity. The viscosity of the solvent, deionised water, was equal to 1.0073 mPa s. At a concentration of 0.1% (w/w), the specific viscosities range between 1.01 and 1.00, implying that the solute had a minor effect on the viscosity of the solution. At 0.7% (w/w) protein, the specific viscosities of PPC and GLB-RF are 1.11 and 1.09, respectively. This is higher than the viscosity measured for the ALB-RF (1.07). At the highest protein concentration of 2.0% (w/w) the specific viscosity differences become more pronounced, with 1.38 and 1.36 for PPC and GLB-RF, and 1.23 for ALB-RF, respectively. The higher specific viscosities of PPC and GLB-RF can be attributed to the globulins and its ability to form aggregates with a high specific volume. The ALB-RF displays a lower increase in viscosity, which implies that it occupies less volume and has a lower tendency to form protein aggregates.

3.2. Interfacial properties of the pea protein fractions

3.2.1. Adsorption behaviour

The interfacial properties were evaluated using a drop tensiometer, and the protein adsorption behaviour is presented in Fig. 4A. All samples had an immediate increase of surface pressure at the start of the experiment. PPC started at 8 mN/m, followed by a continuous increase up to 25 mN/m. The ALB-RF started at the same surface pressure of 8 mN/m, but showed a slower increase compared to PPC with a final surface pressure of 17 mN/m after 3 h. The GLB-RF had the lowest initial surface pressure of 4 mN/m, but increased rapidly, and followed the curve of the PPC from 80 s onwards to 24 mN/m. Albumins showed a faster adsorption on the air-water interface compared to globulins in the initial 10 s, but afterwards the globulins are able to reach higher values. These differences in initial adsorption rate are most likely related to the differences in molecular weights of the proteins, as the main albumins PA1 and PA2 are between 48 and 53 kDa and the globulins vary from 170 to 380 kDa. Smaller proteins can diffuse faster towards the interface and have lower surface adsorption energy, which explains a faster adsorption of albumins compared to the larger globulins (Dickinson, 2011; Yang, Thielen, et al., 2020). The lower charge of albumins also tends to promote faster adsorption, as albumins and globulins had a zeta-potential of −2.0 and −10.3 mV, respectively. Lower surface charges result in lower repulsive forces between adsorbed proteins, as a result proteins can approach each other closer, which could lead to a higher packing density of the smaller albumins. Therefore, albumins are expected to adsorb faster at the interface in the initial phase (Berton-carabin, Sagis, & Schroën, 2018), and the same proteins are likely to be responsible for the fast initial adsorption phase of the PPC. Afterwards, the globulins are responsible for the further increase of surface pressure for PPC. The nature of these interfaces was further evaluated by applying dilatational deformations.

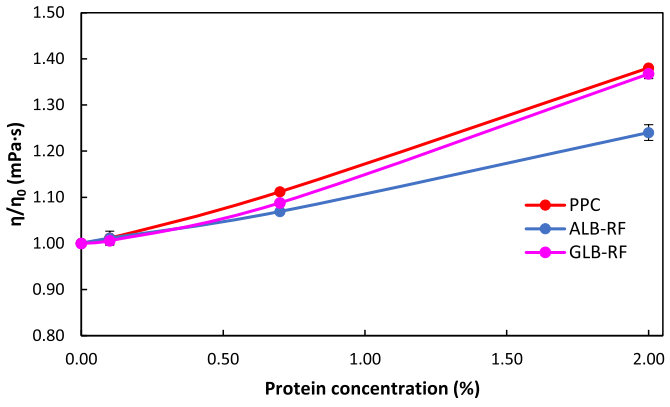

Fig. 3. Viscosities of solutions of the pea protein concentrate (PPC), albumin-rich fraction (ALB-RF) and globulin rich fraction (GLB-RF) relative to the solvent viscosity (η/η_0), measured by capillary viscometry at three concentrations (0.1, 0.7 and 2.0% (w/w)) at pH 7.0. Samples were measured in duplicate and standard deviations are shown as error bars.

3.2.2. Dilatational rheology

First, frequency sweeps were performed on the pea protein-stabilised interfacial films The E_d' versus frequency (data not shown) revealed a power-law behaviour and a weak frequency-dependency, which was quantified using equation (3).

$$E_d' \sim \omega^n \tag{3}$$

Here, ω is the frequency (s^{-1}), and the n-value describes the frequency-dependency. An n-value of 0.5 was previously correlated to an interfacial film, where the elasticity was predominantly determined by mass exchange of surface stabiliser between the bulk and the interface, as expected to occur for small molecular surfactants with the absence of in-plane interactions (Lucassen & Van Den Tempel, 1972). The n-value of PPC, ALB-RF and GLB-RF were estimated 0.20, 0.13, and 0.13, respectively. These values are much lower than 0.5, and suggest that other phenomena are dictating the elasticity of the interface, such as momentum transfer between the interface and bulk, and in-plane interactions between the proteins at the interface (Sagis et al., 2019).

To further assess the mechanical properties of the interfacial films, amplitude sweeps were performed by subjecting the protein-stabilised interfaces to amplitude deformations increasing from 3 to 30%, at a fixed frequency of 0.02 Hz, and the resulting surface dilatational moduli are presented in Fig. 4B. All interfaces had a higher E_d' (storage modulus) compared to E_d' (loss modulus), resulting in a tanδ' = E_d"/E_d' of below 1, revealing elastic-dominated and solid-like behaviour (Jaishankar & McKinley, 2013; J.; Yang, Li, et al., 2020). The E_d' of PPC-stabilised interface declined slightly from 33 to 26 mN/m, when increasing the amplitude from 3 to 30%. A comparable behaviour was found for the GLB-RF-stabilised interface with moduli decreasing from 38 to 28 mN/m. The moduli for both PPC- and GLB-RF-stabilised interfaces were found to be (nearly) independent of the applied deformations, especially compared to the ALB-RF-stabilised interfaces. The ALB-RF-stabilised interface had remarkably high moduli at low deformations, decreasing from 82 to 38 mN/m upon increasing the deformation amplitude.

Deformations in the nonlinear viscoelastic (NLVE) regime result in the presence of higher-order harmonics in the Fourier spectrum of the stress response. These higher harmonics are neglected, when the surface dilatational moduli are obtained from only the first harmonic of the Fourier spectrum, as is the case for moduli shown in Fig. 4B. Therefore, analysing only the first harmonic moduli in the NVLE regime is of limited value. Higher harmonics can be included in the analysis by plotting the surface pressure over the deformation $(A\text{-}A_0)/A_0$ in so-called Lissajous plots (Ewoldt, Hosoi, & McKinley, 2008).

3.2.3. Lissajous plots

The PPC- and GLB-RF-stabilised interfaces showed nearly identical Lissajous plots (Fig. 5). At 5% deformation, the Lissajous plots were narrow and nearly symmetric, and suggest near linear viscoelastic behaviour. The plots became asymmetric at higher deformations, for instance at 30% deformation, showing different behaviour in extension and compression of the interfacial area. At the start of the extension (bottom left corner, deformation of −0.35), the surface pressure increased steeply, which indicated a predominantly elastic response. After this point, the curve started to flatten, suggesting gradual softening and disruption of the interfacial microstructure. Consequently, the

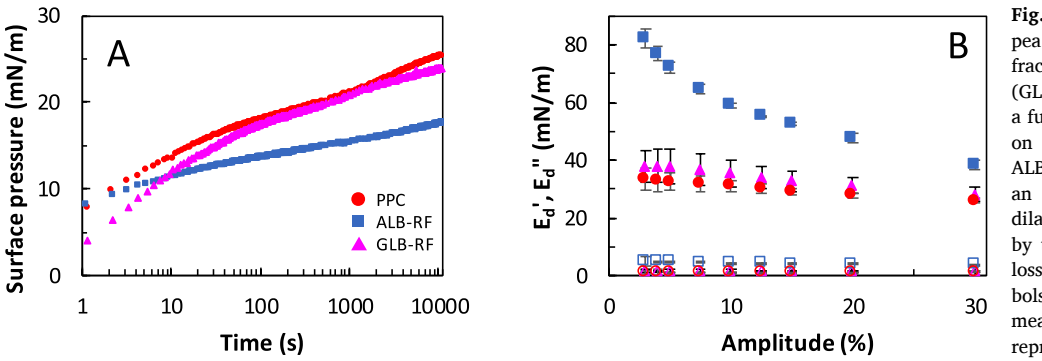

Fig. 4. (A) Surface pressure isotherms of the pea protein concentrate (PPC), albumin-rich fraction (ALB-RF) and globulin-rich fraction (GLB-RF). (B) Surface dilatational moduli as a function of deformation amplitude applied on air-water interfaces stabilised by PPC, ALB-RF and GLB-RF at pH 7.0, measured at an oscillatory frequency of 0.02 Hz. The dilatational storage modulus (Ed') are shown by the closed symbols, and the dilatational loss modulus (Ed") are shown as open symbols. For figure A, the samples were measured at least in triplicate, and one representative curve is shown. For figure B, the samples were measured at least in triplicate and the standard deviations are given in the figure.

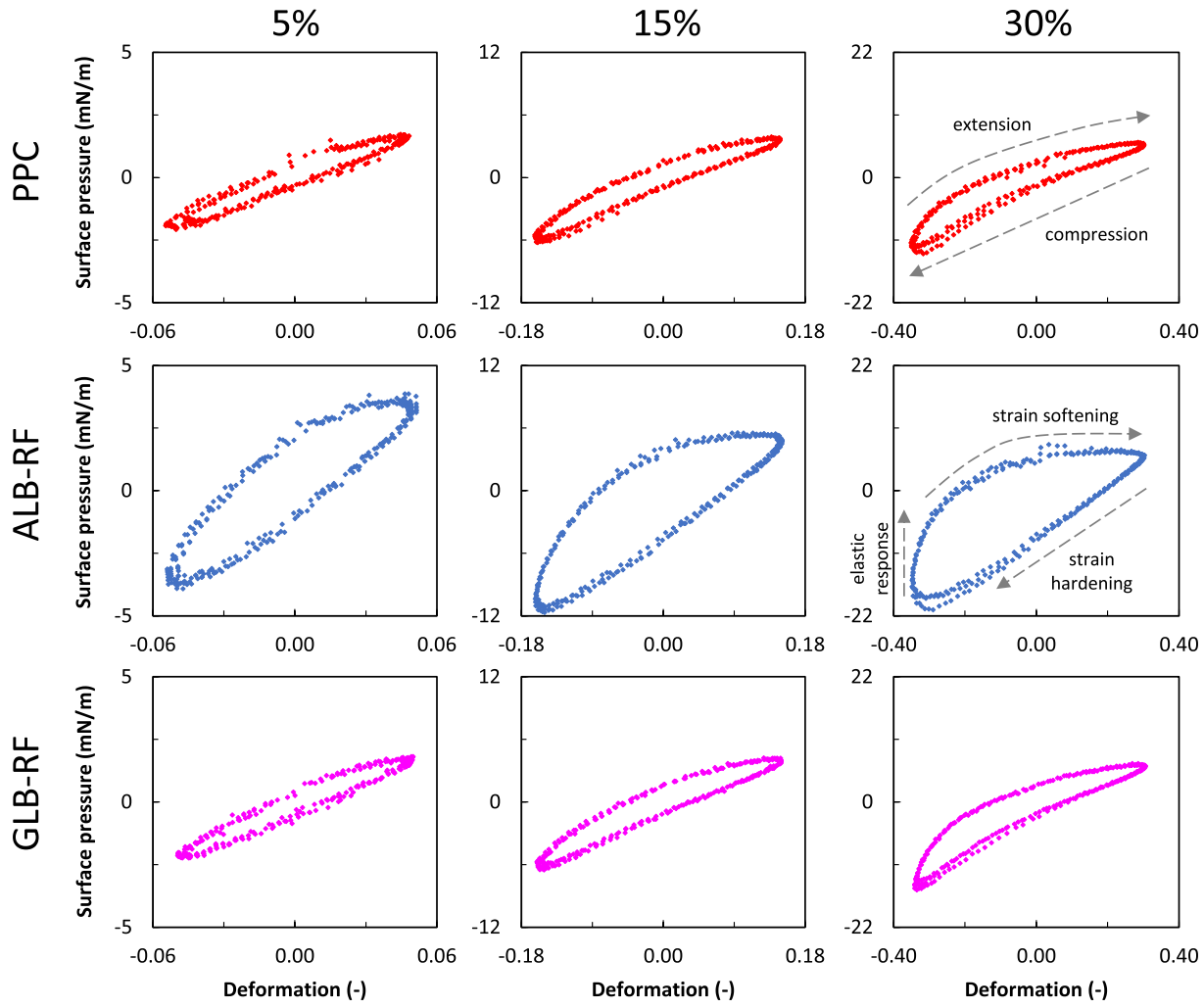

Fig. 5. Lissajous plots of surface pressure as a function of applied deformation (5–30%), obtained from amplitude sweeps of air-water interfaces stabilised by the pea protein concentrate (PPC), albumin-rich fraction (ALB-RF) and globulin-rich fraction (GLB-RF) at pH 7.0. The samples were measured at least in triplicate and one representative plot is shown.

elastic contribution of the response diminishes, whereas the viscous contribution increases, and, finally, results in intra-cycle strain softening in extension. In the compression part of the cycle, the surface pressure showed a steep increase with a higher absolute maximum surface pressure compared to extension, which is known as intra-cycle strain hardening in compression. In previous work, this behaviour was related to the formation of densely clustered regions on the surface that started jamming at such large deformations (J. Yang, Li, et al., 2020).

The asymmetries were even more obviously present in the Lissajous plot of ALB-RF-stabilised interfaces at 30% deformation. Here, we can observe a nearly vertical increase of surface pressure at the start of the extension phase, a zero-slope part at the end of the extension, and a much higher maximum surface pressure of 22 mN/m in compression compared to PPC- and GLB-RF-stabilised interfaces. As a result, the

Lissajous plot of ALB-RF were wider compared to the other two interfaces, suggesting more dissipation of energy upon deformation. The extreme strain softening in extension can also be attributed to a density effect, as the interfacial layer is stretched upon extension. This leads to the dilution of adsorbed proteins, as new proteins are probably not introduced upon extension. Additionally, the increased strain hardening in compression could also be the result of a density effect, where adsorbed proteins are concentrated upon compression, leading to interaction and jamming of the proteins. Asymmetries in the extension and compression cycle of Lissajous plots demonstrate strong in-plane interactions between stabilisers at the interface, which allows the albumins to form a stiff and viscoelastic solid-like interfacial layer, which is disrupted and yields at large deformation. Both the PPC and GLB-RF formed similar interfaces, which were weaker and more easily stretchable interfaces compared to the ALB-RF. The globulins dominated the interfacial properties of the PPC, which was also indicated by the adsorption behaviour (Fig. 4A).

The protein properties of albumins and globulins, as studied in section 3.1., can explain the differences in interfacial layer formation. The albumins are smaller compared to globulins, and also possesses a lower net protein charge (Kornet et al., 2021). As a result, the electrostatic repulsion between albumins at the interface is lower, and more albumins can fit on the interface, as the proteins can closely approach each other. This could strengthen the interactions between the proteins on the surface. Additionally, their smaller size could result in a more efficient coverage of the interface by the albumins. Another explanation can be found in the protein surface hydrophobicity. For albumins from rapeseed, it was shown that two distinct regions exist on the protein surface: a hydrophobic and a hydrophilic one (Ntone et al., 2020), thus resembling an amphiphilic Janus-particle. Unfortunately, such information on the pea protein pea structure is unavailable, but it was demonstrated that albumins from various plant sources showed great similarities in their protein tertiary structure (Souza, 2020). Therefore, it is likely that the pea albumins also have this distinct amphiphilic structure. Such amphiphilicity could allow these proteins to have stronger in-plane interactions on the surface compared to globulins, which have more evenly distributed hydrophobic regions on the protein's surface (Ntone et al., 2020).

3.2.4. Interfacial microstructure

The pea protein-stabilised interfacial films were further evaluated by producing Langmuir-Blodgett films, and were analysed using atomic force microscopy to study the topography of the films (Fig. 6). Surface pressure isotherms obtained from the Langmuir trough can be observed in Fig. S1. The PPC and GLB-RF-stabilised films at a surface pressure of 15 mN/m showed similarities, as both films had larger structures, which were not observed for ALB-RF. These larger structures could be clusters of proteins, to be more specific, of the globulins. The formation of such clusters was also observed for rapeseed proteins (Yang, Faber, et al., 2021). The similarities between the films of PPC and GLB-RF again reveal the dominance of globulins at the air-water interface.

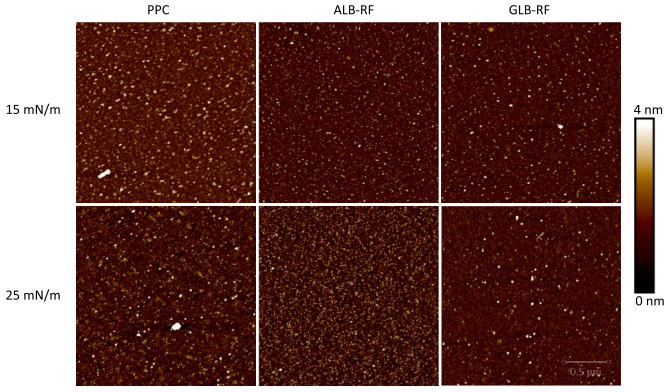

Fig. 6. Atomic Force Microscopy (AFM) images of Langmuir-Blodgett films made from pea protein concentrate (PPC), albumin-rich fraction (ALB-RF) and globulin-rich fraction (GLB-RF) stabilised air-water interfaces. The surface pressure indicates the conditions during film sampling.

The changes in the microstructure of the interface upon deformation were evaluated by further compressing the Langmuir films to a surface pressure of 25 mN/m, before film deposition. For PPC and GLB-RF-stabilised interfacial films, the interfaces remained similar to the films at a lower compression (15 mN/m). This can be linked to formation of a weak and highly stretchable interfacial layer, as shown in the dilatational surface rheology. Due to low in-plane forces between the globulins, these proteins could be pushed out of the interface. We should keep in mind that the AFM only studies the topography of the interface, the larger structures could also be pushed to the other side of the film or become covered at higher compressions. At 25 mN/m, the ALB-RF-stabilised interfacial film was found to be denser and finer compared to the other two interfacial films. This interface closely resembles one shown by whey protein isolate in our previous work (J. Yang, Li, et al., 2020). Here, we suggested that whey proteins were able to form stiff layers with a heterogeneous microstructure, and the pea albumins are able to form such highly interlinked layers as well, as exhibited in the rheology. The strong in-plane interactions between albumins allows the proteins to remain on the surface upon compression, forming such dense microstructures. The heterogeneity in the interfacial microstructure is observed for the films of all three protein fractions, and has been demonstrated for other protein sources, such as whey (Rühs, Affolter, Windhab, & Fischer, 2013) (Gunning et al., 1996), pea (E. B. A. Hinderink, Sagis, Schroen, & Berton-Carabin, 2020) and rapeseed (Yang, Faber, et al., 2021). Such structural arrangement of the proteins can be further analysed using step-dilatations.

3.2.5. Step-dilatational behaviour

The air-water interfacial layers stabilised by the pea protein fractions were subjected to step-dilatations, where the surface area is suddenly compressed or extended. Afterwards, the new surface area was maintained to obtain a relaxation response, which was fitted to a Kohlraus-William-Watts (KWW) stretch exponential coupled with a regular exponential term (Equation (4)) (Williams & Watts, 1969) (Sagis et al., 2019)

$$\gamma(t) = ae^{-(t/\tau_1)^{\beta}} + be^{-t/\tau_2} + c \quad (4)$$

Here, γ is the surface stress (mN/m), t is the time (s), τ_1 is the relaxation time, and β is the stretch exponent. The second term is required to decouple the continuous decrease of surface stress, due to aging of the interface. Here, the characteristic time τ_2 describes this process. The a, b and c are used as fitting parameters. An overview of all parameters can be found in Table S1.

The stretch exponent β in the KWW equation indicates dynamic heterogeneity when the β-value is < 1. This implies there are local variations in the relaxation response, which result in a wide spectrum of relaxation times (Phillips, 1996). The β-values of the pea protein-stabilised interfaces were found to be between 0.55 and 0.74

Table 3
Stretch component β and characteristic relaxation time τ_1 obtained from step-dilatation experiments of air-water interfaces stabilised by pea protein concentrate (PPC), albumin-rich fraction (ALB-RF) and globulin-rich fraction (GLB-RF) at pH 7.0. Values are presented as mean ± standard deviation; means within a column with the same superscript letter are not significantly different ($p > 0.05$).

Pea protein fraction	Compression		Extension	
	β	τ_1	β	τ_1
PPC	0.67 ± 0.07^{a}	$4.6 \pm 1.5^{a,b}$	0.58 ± 0.04^{a}	8.3 ± 2.6^{a}
ALB-RF	0.74 ± 0.05^{a}	6.4 ± 0.9^{b}	0.55 ± 0.02^{a}	6.2 ± 0.8^{a}
GLB-RF	0.63 ± 0.08a	4.1 ± 0.9^{a}	0.56 ± 0.04^{a}	8.4 ± 2.5^{a}

(Table 3), revealing dynamic heterogeneity (Sagis et al., 2019). The heterogeneous microstructure (Fig. 6) could cause this type of response, which was previously confirmed for disordered (or heterogeneous) solids (Klafter & Shlesinger, 1986; Sagis et al., 2019). From the results of the interfacial properties, we conclude that all that these three pea protein fractions form comparable heterogeneous structures at the air-water interface, which was also reflected in comparable relaxation times (τ_1). The ALB-RF-stabilised interface also had a slightly higher β-value upon compression compared to one stabilised by GLB-RF. This difference could be related to the stiffer interfacial films formed by albumins. The AFM images (Fig. 6), especially at 25 mN/m, showed the formation of a denser and probably more homogeneous structure by albumins, which could cause the β-value upon compression to increase compared to globulin-stabilised interfaces.

3.2.6. Summary on interfacial properties

The albumin protein in ALB-RF and globulin proteins in GLB-RF are markedly different from a molecular perspective, as albumins are smaller and less charged than globulins. As a result, albumins are able to rapidly adsorb at the air-water interface, and have strong attractive in-plane protein-protein interactions. These result in a stiff and dense interfacial layer, as shown by both surface rheology and microstructure imaging. In contrast, globulins form highly aggregated structures with high charges, leading to a lower surface activity, and also weaker in-plane interactions at the interface. The highly aggregated structures and charged structures lead to a less dense interfacial film (as shown by AFM), which is substantially weaker compared to the albumin films. The interface stabilising properties of the mildly fractionated mixture (PPC) were mainly dominated by the globulins, which was expected as globulins are more abundantly present than albumins. Here, we show how the molecular properties of these pea proteins are controlling the interface stabilising properties, which could also affect the macroscopic properties, such as foaming and emulsification, which will be discussed in the following sections.

3.3. Foaming properties of the pea protein fractions

Foams stabilised by the pea proteins were analysed for their foaming ability (overrun and air bubble size) and stability (half-life time). The ALB-RF were far more superior in foaming ability compared to PPC and GLB-RF, as the overrun (% foam volume generated, Equation (1)) was 258% for ALB-RF, while PPC and GLB-RF only had an overrun of 81 and 61%, respectively (Fig. 7A). Albumins were also able to form smaller air bubbles compared to the other two samples (Fig. 7B), as albumins form four times smaller air bubbles compared to the globulins. This difference in overrun and bubble size could be attributed to the differences in the surface activity (Fig. 4), as albumin is more surface active in the first 10 s of adsorption. Additionally, the albumins form stiffer interfacial layers, and could allow the formation and retention of a higher foam volume. Weaker interfacial layers formed by globulins could result in the immediate collapse of the air bubble, thus resulting in a lower overrun. The albumins in the PPC mixture seemed to have increased the overrun and decreased the air bubble size slightly, which suggests the contribution of albumins on the air bubble formation. This is also reflected in the adsorption behaviour, as the PPC exhibited a faster increase in the initial adsorption phase compared to globulins, suggesting a contribution of albumins to the initial adsorption phase and the air bubble formation. As the absolute number of albumin molecules is lower in the PPC, the foam ability is lower compared to the ALB-RF-stabilised foams.

The foam stability was assessed by comparing the foam volume half-life time (time where foam volume decays by half) (Fig. 7C). The ALB-RF stabilised foams showed a half-life time of 272 min, while the PPC and GLB-RF showed substantially lower half-life times of 14 and 70 min, respectively. The remarkably stable albumin-stabilised foams are the result of the small air bubble size and the stiff interfacial layer around this air bubble. Generally, small air bubbles increase the total interfacial area in the foam, thereby increasing the liquid captured around the bubbles and in the foam, thus slowing down drainage. Also, small air bubbles (with a narrow size distribution) decrease the disproportionation of gas between air bubbles. The stiff solid-like interfacial layers formed by albumins could further slowdown the disproportionation and increase the resistance of air bubbles against coalescence. A combination of these factors resulted in the exceptionally high foam stability of albumin-stabilised foams, which showed a similar air bubble size and foam stability as whey protein-stabilised foams at similar conditions in our previous work (Yang, Roozalipour, et al., 2021). Pea albumins, often discarded in fractionation processes, display great potential as a foaming agent.

3.4. Emulsifying properties of the pea protein fractions

The emulsifying properties of the pea protein fractions were studied at protein concentrations of 0.7% and 2% (w/w). A protein-poor and -rich regime was previously established for protein-stabilised emulsions, where the oil droplet size (determined as droplet diameter) decreased with higher protein concentration, as more protein was available to stabilise the generated interface during droplet break-up in the homogeniser. Above a certain protein content, the droplet size is independent of the protein concentration, also known as the protein-rich regime. For this study, the emulsifying properties were evaluated at the boundary of the protein-poor and -rich regime, also known as the critical protein concentration. Based on previously published work on pea protein emulsions, we chose a protein content of 0.7% (w/w) (Hinderink et al., 2019). A protein content in the protein-rich regime was also studied, which was 2% (w/w).

Emulsions with 10% (w/w) oil were studied for the average droplet

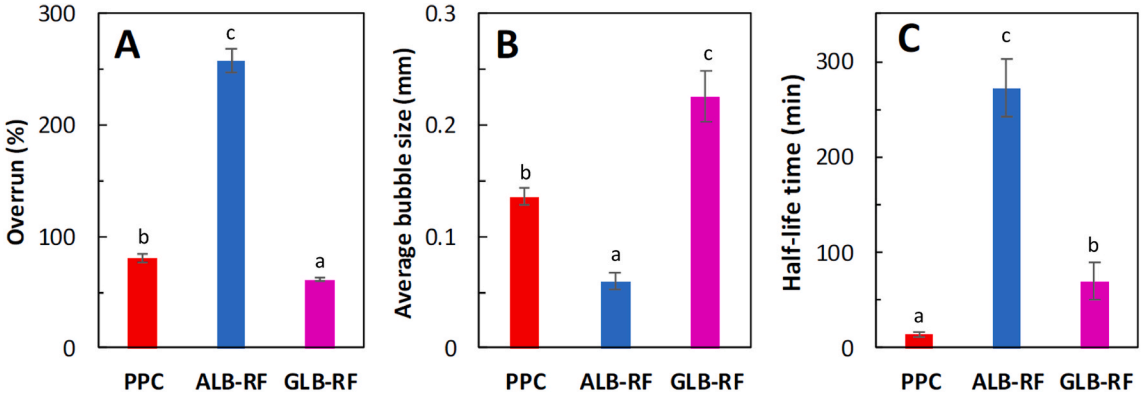

Fig. 7. The overrun (A), average air bubble size (B), and foam volume half-life time (C) of foams stabilised using the pea protein concentrate (PPC), albumin-rich fraction (ALB-RF) and globulin-rich fraction (GLB-RF) at pH 7.0. The samples were measured in triplicate and the standard deviations are given in the figure.

size ($d_{3,2}$) directly after emulsion preparation, and after 7 days of storage (Table 4). In the protein-rich regime at 2% protein (w/w), PPC, ALB-RF and GLB-RF formed emulsions with droplet sizes between 0.50 and 0.55 μm. Potential flocculates were broken down by addition of sodium dodecyl sulphate (SDS), as the SDS replaces the proteins at the surface, introducing a high surface charge, thereby breaking up flocculated droplets. The emulsions formed with 2% (w/w) protein had a similar droplet size after addition of SDS, which suggested that the oil droplets are stable against flocculation. After 7 days, the droplet sizes remained constant, demonstrating stability against coalescence and flocculation for at least 7 days.

At a lower concentration of 0.7%, more distinct differences between the pea protein stabilised emulsions are present. As the droplet sizes of ALB-RF-stabilised emulsions were about three times larger compared to PPC and GLB-RF-stabilised emulsions. The emulsions at these concentrations can be analysed more precisely with the droplet size distribution graphs (Fig. 8). Both PPC- and GLB-RF-stabilised emulsions had a similar size distribution with a peak at 1 μm. Addition of SDS resulted in an overlapping graph, indicating the absence of flocculation. The ALB-RF-stabilised emulsions showed a different size distribution with two peaks, the first peak between 0.3 and 3 μm, and a second peak between 3 and 30 μm. The second peak disappeared upon addition of SDS, which indicates flocculation of oil droplets stabilised by ALB-RF. The single droplet size of ALB-RF-stabilised oil droplets was still larger compared to those of PPC and GLB-RF. Albumins were found to be less effective in oil droplet stabilisation upon emulsion formation, and protected the droplets less against flocculation. The flocculation could occur due to a lower net protein charge of the albumins compared to the globulins (Kornet et al., 2021). This will result in a lower surface charge around the oil droplets, as the proteins are on the outer layer of the droplets. Consequently, less electrostatic repulsion is present between the oil droplets, leading to droplet flocculation. Also, the lower protein net charge could allow more albumins to fit on the interface, due to less electrostatic repulsion between the proteins. As more proteins can fit on the interface, more proteins would be required to stabilise the interface. This point is proven by increasing the protein content to 2% (w/w) into the protein-rich regime, where the albumins give stable emulsion droplets, similar to globulin-stabilised emulsions. A higher number of proteins on the surface could have increased the overall surface charge of the droplet, as the ALB-RF-stabilised emulsions at 2% (w/w) did not show flocculation.

Table 4
Average droplet size ($d_{3,2}$) of 10% (w/w) oil-in-water emulsions stabilised by 0.7 or 2% (w/w) protein concentration of pea protein concentrate (PPC), albumin-rich fraction (ALB-RF) and globulin-rich fraction (GLB-RF) at pH 7.0. The overall droplet size was studied directly after emulsion preparation, and after 7 days of storage at 4 °C. The single droplet size was also studied by breaking up potential flocculates using SDS. Values are presented as mean ± standard deviation; means within a column with the same superscript letter are not significantly different ($p > 0.05$).

Time	Pea protein fraction	0.7% (w/w) protein		2% (w/w) protein	
		Overall droplet size (μm)	Single droplet size (μm)	Overall droplet size (μm)	Single droplet size (μm)
Day 0	**PPC**	0.72 ± 0.03^{a}	0.69 ± 0.02^{a}	0.50 ± 0.04^{a}	0.49 ± 0.01^{a}
	ALB-RF	2.04 ± 0.10^{b}	0.83 ± 0.04^{b}	0.51 ± 0.04^{a}	0.49 ± 0.03^{a}
	GLB-RF	0.71 ± 0.04^{a}	0.67 ± 0.03^{a}	0.55 ± 0.02^{a}	0.55 ± 0.02^{b}
Day 7	**PPC**	0.69 ± 0.04^{a}	0.64 ± 0.03^{a}	0.57 ± 0.02^{a,b}	0.55 ± 0.02^{b}
	ALB-RF	3.78 ± 0.14^{c}	1.99 ± 0.33^{c}	0.58 ± 0.02^{b}	0.59 ± 0.02^{b}
	GLB-RF	0.75 ± 0.03^{a}	0.70 ± 0.05^{a}	0.50 ± 0.02^{a}	0.51 ± 0.02^{a}

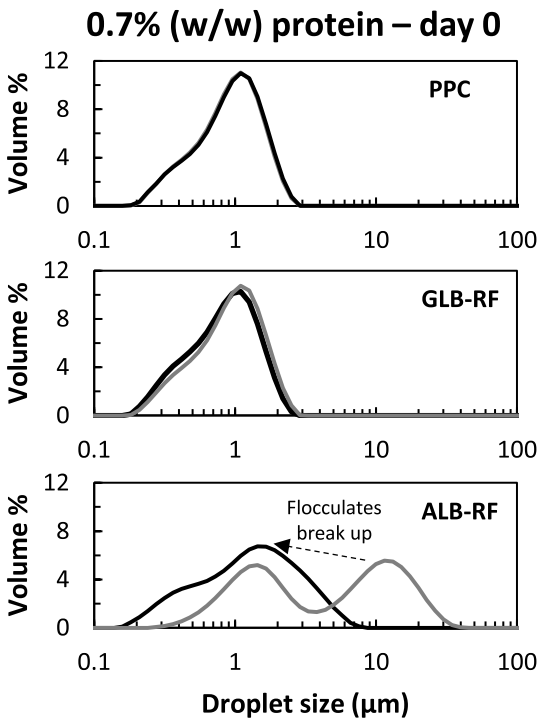

Fig. 8. Droplet size distribution of 10% (w/w) oil-in-water emulsions prepared from pea protein concentrate (PPC), albumin-rich fraction (ALB-RF) and globulin-rich fraction (GLB-RF) with 0.7% (w/w) protein at pH 7.0, directly after emulsion preparation (grey line). The size distribution of single droplets after breaking up flocculates with Sodium Dodecyl Sulphate (SDS) were also shown (black line). The samples were prepared in duplicate and each replicate is measured in triplicate. A representative size distribution was shown.

At 0.7% (w/w), the pea globulins are more effective in stabilising emulsions, and are responsible for the comparable stability of PPC-stabilised emulsions, thus suggesting that the globulins dominated the emulsifying properties. The pea protein globulins (legumin and vicilin) were previously described as surface active molecules, which were able to stabilise the oil-water interface effectively (Barac et al., 2010; E. B.; Hinderink et al., 2019). The pea globulins are larger in molecular weight (170–380 kDa) compared to pea albumins (10–53 kDa) (Barać, Pešić, Stanojević, Kostić, & Čabrilo, 2015; Croy et al., 1980; Higgins et al., 1986), and the globulins also form aggregates in the bulk, as demonstrated for our samples in a previous work (Kornet et al., 2020). The large globulins could contribute to a thicker layer around the oil droplet, which has a sufficiently high surface charge to avoid the droplets from aggregating into flocculates.

The emulsions with a protein content of 0.7% (w/w) were also studied for their stability after 7 days of storage. The PPC- and GLB-RF stabilised emulsions had coinciding $d_{3,2}$-values and droplet size distribution graphs (data not shown) after 7 days. Slight differences can be observed in the droplet size distribution graph of the ALB-RF-stabilised emulsions (Fig. 9). After 7 days of storage, droplets of around 1.5 μm were reduced (left peak), while the larger flocculates of around 10 μm increased to around 25 μm (right peak), revealing a continuous flocculation of the emulsion droplets during the storage period. After addition of SDS, we also observed a slight shift of the single droplet size towards the right, which is also reflected in a $d_{3,2}$ increase from 0.83 to 1.99 μm after 7 days of storage. An increase of the single droplet size indicates two instability phenomena, coalescence of emulsion droplets or irreversible aggregation of the droplets that could not be broken up after addition of SDS. The irreversible flocculation was confirmed using microscopy (Fig. 9), as several larger flocculates were observed among many single droplets.

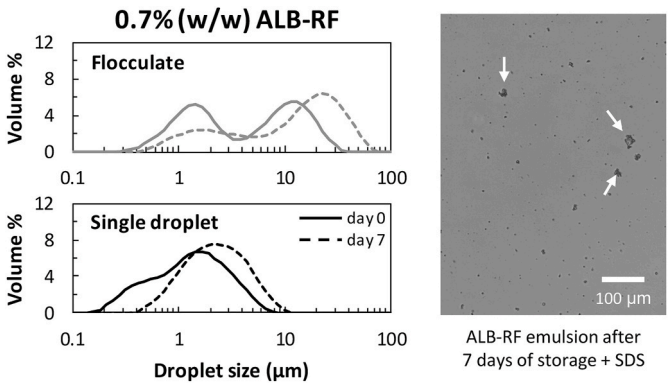

Fig. 9. Droplet size distribution of 10% (w/w) oil-in-water emulsions prepared from albumin-rich fraction (ALB-RF) with 0.7% (w/w) protein at pH 7.0, directly after emulsion preparation (solid line), and after 7 days of storage at 4 °C (dotted line). Single droplets were also studied after breaking up flocculates. The samples were prepared in duplicate and each replicate is measured in triplicate. A representative size distribution was shown. A microscopy image of an ALB-RF-stabilised emulsion after 7 days storage with addition of SDS was also shown. The arrows indicate irreversibly aggregated flocculates.

Another studied emulsion stability property was creaming, which was not visible after 7 days of storage at 4 °C for emulsions stabilised with 2% protein (w/w) (data not shown). At 0.7% (w/w), only the ALB-RF stabilised emulsions showed creaming, which was measured and converted into a creaming factor (see equation (2)). Directly after preparation, the ALB-RF showed no creaming (creaming factor of 0%), but after 4–5 h a transparent layer was observed at the bottom of the tubes. After 24 h, the creaming factor was 65%, and further increased to 74% after 7 days of storage. According to Stokes law, two major parameters play a role in this case, which are the droplet size and viscosity. The ALB-RF protein solution only had a slightly lower viscosity (1.7–3.9%) compared to PPC and GLB-RF (Fig. 3). Therefore, large flocculated droplets seem to play a major role in the creaming of the droplets. At higher concentrations, the albumins could form small droplets that were stable against flocculation, and thus against creaming.

In summary, we proved that pea globulins are more effective in stabilising emulsions at 0.7% (w/w) protein than albumins. Another important finding is the fact that an extensively purified pea protein isolate (GLB-RF) showed similar emulsion properties as a mildly purified pea protein concentrate (PPC). For the preparation of stable emulsions, a PPC could already be sufficient.

4. Conclusion

Aqueous fractionation from pea flour yielded three different pea protein fractions with significantly different functionalities. The small size and lower net protein charge of albumins led to high in-plane interactions at the air-water interface, thus resulting in a stiff and cohesive interfacial layer. Such a strong interfacial layer around the air bubble could explain a four times higher foam ability, and almost twenty times higher foam stability compared to the globulin-dominated fractions. The poor foaming properties of globulins could be related to the formation of a weak and stretchable interface, caused by a more aggregated state and higher net protein charge. It is worth mentioning that the foaming properties of albumin-stabilised foams are remarkably similar to whey protein isolate (Yang, Roozalipour, et al., 2021). On the other hand, the pea protein concentrate (PPC) and globulin-rich fraction (GLB-RF) contained mainly globulins, which led to smaller emulsion droplets with higher stability against flocculation compared to the albumin-rich fraction (ALB-RF). This difference in functionality can be attributed to the molecular properties, as the globulins are larger and more highly charged, leading to a droplet with a thicker interfacial layer and a higher surface charge.

In this work, we showed that the plant protein fractionation method can be tuned to obtain protein ingredients with either promising foaming or emulsifying properties. Albumins can be used as a foam stabiliser, while globulins can be used as an emulsion stabiliser. In a mild fractionation process, where albumins and globulins were co-extracted, the globulins seemed to dominate the functional properties, thus resulting in good oil droplet stabilisation. A mild fractionation method consists of fewer processing steps compared to conventional protein fractionation methods, and may optimize pea resource efficiency by also using by-products in a fractionation process. Moreover, our work shows that fractionation methods can be optimized to yield pea protein fractions that have the potential to function as either foaming or emulsifying agents in food products.

Author statement

Remco Kornet: Conceptualization, Methodology, Investigation, Validation, Visualization, Writing – Original Draft. **Jack Yang:** Conceptualization, Methodology, Investigation, Validation, Visualization, Writing – Original Draft. **Paul Venema:** Supervision, Writing – Review & Editing. **Erik van der Linden:** Writing – Review & Editing, Funding Acquisition. **Leonard Sagis:** Conceptualization, Methodology, Supervision, Writing – Review & Editing.

Declaration of competing interest

We confirm that this work is original and has not been published or presented elsewhere in part or in entirety and is not under consideration by another journal. All the authors have approved the manuscript and agree with submission to your esteemed journal. We have read and understood your journal's policies, and we believe that neither the manuscript nor the study violates any of these. The authors have declared that no competing interests exist.

Acknowledgements

The authors want to thank Maria Georgopoulou for doing exploratory measurements that contributed to the direction of this study. They also thank Helene Mocking-Bode for her help with fractionation and Maud Meijers for support with size exclusion chromatography. The authors have declared that no competing interest exists. The project is funded by TiFN, a public-private partnership on precompetitive research in food and nutrition. The public partners are responsible for the study design, data collection and analysis, decision to publish, and preparation of the manuscript. The private partners have contributed to the project through regular discussion. This research was performed with additional funding from the Netherlands Organisation for Scientific Research (NWO), and The Top Consortia for Knowledge and Innovation of the Dutch Ministry of Economic Affairs (TKI). NWO project number: ALWTF.2016.001.

Appendix A. Supplementary data

Supplementary data to this article can be found online at https://doi.org/10.1016/j.foodhyd.2021.107456.

References

Arntfield, S., & Murray, E. (1981). The influence of processing parameters on food protein functionality I. Differential scanning calorimetry as an indicator of protein denaturation. *Canadian Institute of Food Science and Technology Journal, 14*(4), 289–294.

Assatory, A., Vitelli, M., Rajabzadeh, A. R., & Legge, R. L. (2019). Dry fractionation methods for plant protein, starch and fiber enrichment: A review. *Trends in Food Science & Technology, 86*, 340–351.

Barac, M., Cabrilo, S., Pesic, M., Stanojevic, S., Zilic, S., Macej, O., et al. (2010). Profile and functional properties of seed proteins from six pea (Pisum sativum) genotypes. *International Journal of Molecular Sciences, 11*(12), 4973–4990.

Barać, M. B., Pešić, M. B., Stanojević, S. P., Kostić, A.Ž., & Čabrilo, S. B. (2015). Techno-functional properties of pea (Pisum sativum) protein isolates-a review. *Acta Periodica Technologica, 46*, 1–18.

Berton-carabin, C. C., Sagis, L., & Schroën, K. (2018). Formation , structure , and functionality of interfacial layers in food emulsions. *Annual Review of Food Science and Technology, 9*, 551–587.

Boukid, F., Rosell, C. M., & Castellari, M. (2021). Pea protein ingredients: A mainstream ingredient to (re) formulate innovative foods and beverages. *Trends in Food Science & Technology, 110*, 729–742.

Boye, J., Zare, F., & Pletch, A. (2010). Pulse proteins: Processing, characterization, functional properties and applications in food and feed. *Food Research International, 43*(2), 414–431.

Burger, T. G., & Zhang, Y. (2019). Recent progress in the utilization of pea protein as an emulsifier for food applications. *Trends in Food Science & Technology, 86*, 25–33.

Casey, R., Sharman, J. E., Wright, D. J., Bacon, J. R., & Guldager, P. (1982). Quantitative variability in pisum seed globulins: Its assessment and significance. *Plant Foods for Human Nutrition, 31*(4), 333–346.

Croy, R., Gatehouse, J. A., Tyler, M., & Boulter, D. (1980). The purification and characterization of a third storage protein (convicilin) from the seeds of pea (Pisum sativum L.). *Biochemical Journal, 191*(2), 509–516.

Dickinson, E. (2011). Mixed biopolymers at interfaces: Competitive adsorption and multilayer structures. *Food Hydrocolloids, 25*(8), 1966–1983.

Ewoldt, R. H., Hosoi, A. E., & McKinley, G. H. (2008). New measures for characterizing nonlinear viscolasticity in large amplitude oscillatory shear (Laos). *Journal of Rheology, 52*(6), 2008.

Geerts, M. E. J., Mienis, E., Nikiforidis, C. V., van der Padt, A., & van der Goot, A. J. (2017). Mildly refined fractions of yellow peas show rich behaviour in thickened oil-in-water emulsions. *Innovative Food Science & Emerging Technologies, 41*, 251–258.

Ghumman, A., Kaur, A., & Singh, N. (2016). Functionality and digestibility of albumins and globulins from lentil and horse gram and their effect on starch rheology. *Food Hydrocolloids, 61*, 843–850.

Gunning, A. P., Wilde, P. J., Clark, D. C., Morris, V. J., Parker, M. L., & Gunning, P. A. (1996). Atomic force microscopy of interfacial protein films. *Journal of Colloid and Interface Science, 183*(2), 600–602.

Higgins, T., Chandler, P., Randall, P., Spencer, D., Beach, L., Blagrove, R., et al. (1986). Gene structure, protein structure, and regulation of the synthesis of a sulfur-rich protein in pea seeds. *Journal of Biological Chemistry, 261*(24), 11124–11130.

Hinderink, E. B., Münch, K., Sagis, L., Schroën, K., & Berton-Carabin, C. C. (2019). Synergistic stabilisation of emulsions by blends of dairy and soluble pea proteins: Contribution of the interfacial composition. *Food Hydrocolloids, 97*, 105206.

Hinderink, E. B. A., Sagis, L., Schroen, K., & Berton-Carabin, C. C. (2020). Behavior of plant-dairy protein blends at air-water and oil-water interfaces. *Colloids and Surfaces B: Biointerfaces, 192*, 111015.

Jaishankar, A., & McKinley, G. H. (2013). Power-law rheology in the bulk and at the interface: Quasi-properties and fractional constitutive equations. *Proceedings of the Royal Society A: Mathematical, Physical & Engineering Sciences, 469*(2149), 20120284.

Karaca, A. C., Low, N., & Nickerson, M. (2011). Emulsifying properties of chickpea, faba bean, lentil and pea proteins produced by isoelectric precipitation and salt extraction. *Food Research International, 44*(9), 2742–2750.

Kimura, A., Fukuda, T., Zhang, M., Motoyama, S., Maruyama, N., & Utsumi, S. (2008). Comparison of physicochemical properties of 7S and 11S globulins from pea, fava bean, cowpea, and French bean with those of soybea – French bean 7S globulin exhibits excellent properties. *Journal of Agricultural and Food Chemistry, 56*(21), 10273–10279.

Klafter, J., & Shlesinger, M. F. (1986). On the relationship among three theories of relaxation in disordered. *Proceedings of the National Academy of Sciences of the United States of America, 83*(4), 848–851.

Kornet, R., Veenemans, J., Venema, P., Goot, A. J.v. d., Meinders, M., Sagis, L., et al. (2021). Less is more: Limited fractionation yields stronger gels for pea proteins. *Food Hydrocolloids, 112*, 106285.

Kornet, R., Venema, P., Nijsse, J., Linden, E.v. d., Goot, A. J.v. d., & Meinders, M. (2020). Yellow pea aqueous fractionation increases the specific volume fraction and viscosity of its dispersions. *Food Hydrocolloids, 99*, 105332.

Lam, A. C. Y., Can Karaca, A., Tyler, R. T., & Nickerson, M. T. (2016). Pea protein isolates: Structure, extraction, and functionality. *Food Reviews International, 34*(2), 1–22.

Lie-Piang, A., Braconi, N., Boom, R. M., & van der Padt, A. (2021). Less refined ingredients have lower environmental impact–A life cycle assessment of protein-rich ingredients from oil-and starch-bearing crops. *Journal of Cleaner Production*, 126046.

Lucassen, J., & Van Den Tempel, M. (1972). Dynamic measurements of dilational properties of a liquid interface. *Chemical Engineering Science, 27*(6), 1283–1291.

Lu, B. Y., Quillien, L., & Popineau, Y. (2000). Foaming and emulsifying properties of pea albumin fractions and partial characterisation of surface-active components. *Journal of the Science of Food and Agriculture, 80*(13), 1964–1972.

Mession, J.-L., Sok, N., Assifaoui, A., & Saurel, R.m. (2013). Thermal denaturation of pea globulins (pisum sativum L.). Molecular interactions leading to heat-induced protein aggregation. *Journal of Agricultural and Food Chemistry, 61*(6), 1196–1204.

Möller, A. C., van der Padt, A., & van der Goot, A. J. (2020). From raw material to mildly refined ingredient–Linking structure to composition to understand fractionation processes. *Journal of Food Engineering*, 110321.

Ntone, E., van Wesel, T., Sagis, L. M. C., Meinders, M., Bitter, J. H., & Nikiforidis, C. V. (2020). Adsorption of rapeseed proteins at oil/water interfaces. Janus-like napins dominate the interface. *Journal of Colloid and Interface Science, 583*, 459–469.

O'Kane, F. E., Happe, R. P., Vereijken, J. M., Gruppen, H., & van Boekel, M. A. (2004). Characterization of pea vicilin. 1. Denoting convicilin as the α-subunit of the Pisum vicilin family. *Journal of Agricultural and Food Chemistry, 52*(10), 3141–3148.

Park, S. J., Kim, T. W., & Baik, B. K. (2010). Relationship between proportion and composition of albumins, and in vitro protein digestibility of raw and cooked pea seeds (Pisum sativum L.). *Journal of the Science of Food and Agriculture, 90*(10), 1719–1725.

Phillips, J. C. (1996). Stretched exponential relaxation in molecular and electronic glasses. *Reports on Progress in Physics, 59*, 1133–1207.

Rühs, P. A., Affolter, C., Windhab, E. J., & Fischer, P. (2013). Shear and dilatational linear and nonlinear subphase controlled interfacial rheology of β-lactoglobulin fibrils and their derivatives. *Journal of Rheology, 57*(3), 1003–1022.

Sagis, L. M. C., Liu, B., Li, Y., Essers, J., Yang, J., Moghimikheirabadi, A., et al. (2019). Dynamic heterogeneity in complex interfaces of soft interface-dominated materials. *Scientific Reports, 9*(1), 1–12.

Schutyser, M. A. I., & van der Goot, A. J. (2011). The potential of dry fractionation processes for sustainable plant protein production. *Trends in Food Science & Technology, 22*(4), 154–164.

Shand, P. J., Ya, H., Pietrasik, Z., & Wanasundara, P. K. J. P. D. (2007). Physicochemical and textural properties of heat-induced pea protein isolate gels. *Food Chemistry, 102*(4), 1119–1130.

Souza, P. F. N. (2020). The forgotten 2S albumin proteins: Importance, structure, and biotechnological application in agriculture and human health. *International Journal of Biological Macromolecules, 164*, 4638–4649.

Sridharan, S., Meinders, M. B., Bitter, J. H., & Nikiforidis, C. V. (2020). Pea flour as stabilizer of oil-in-water emulsions: Protein purification unnecessary. *Food Hydrocolloids, 101*, 105533.

Taherian, A. R., Mondor, M., Labranche, J., Drolet, H., Ippersiel, D., & Lamarche, F. (2011). Comparative study of functional properties of commercial and membrane processed yellow pea protein isolates. *Food Research International, 44*(8), 2505–2514.

Tenorio, A. T., Kyriakopoulou, K. E., Suarez-Garcia, E., van den Berg, C., & van der Goot, A. J. (2018). Understanding differences in protein fractionation from conventional crops, and herbaceous and aquatic biomass-Consequences for industrial use. *Trends in Food Science & Technology, 71*, 235–245.

Williams, G., & Watts, D. C. (1969). Non-symmetrical dielectric relaxation behaviour arising from a simple empirical decay function. *Transactions of the Faraday Society, 66*(1), 80–85.

Yang, J., Faber, I., Berton-Carabin, C. C., Nikiforidis, C. V., van der Linden, E., & Sagis, L. M. C. (2021). Foams and air-water interfaces stabilised by mildly purified rapeseed proteins after defatting. *Food Hydrocolloids, 112*.

Yang, S., Li, X., Hua, Y., Chen, Y., Kong, X., & Zhang, C. (2020). Selective complex coacervation of pea whey proteins with chitosan to purify main 2S albumins. *Journal of Agricultural and Food Chemistry, 68*(6), 1698–1706.

Yang, J., Roozalipour, S. P. L., Berton-Carabin, C. C., Nikiforidis, C. V., van der Linden, E., & Sagis, L. M. (2021). Air-water interfacial and foaming properties of whey protein-sinapic acid mixtures. *Food Hydrocolloids, 112*, 106467.

Yang, J., Thielen, I., Berton-Carabin, C. C., van der Linden, E., & Sagis, L. M. C. (2020). Nonlinear interfacial rheology and atomic force microscopy of air-water interfaces stabilized by whey protein beads and their constituents. *Food Hydrocolloids, 101*, 105466.